Clays and Clay Minerals, 1972, Vol. 20, pp. 217–223. Pergamon Press. Printed in Great Britain

A FERROAN NONTRONITE FROM THE RED SEA GEOTHERMAL SYSTEM

JAMES. L. BISCHOFF
Department of Geological Sciences, University of Southern California, Los Angeles, Calif. 90007, U.S.A.

(*Received* 3 *February* 1972)

Abstract—A smectite rich in ferrous iron and low in aluminum occurs abundantly in the Red Sea Geothermal Deposits, and appear to be forming at present.

Chemical analyses and Mössbauer spectra indicate the mineral is intermediate in composition between nontronite and the as yet undescribed trioctahedral ferrous iron end member.

INTRODUCTION AND OCCURRENCE

THE Red Sea geothermal brine deposits are directly precipitating due to discharge of a hot brine onto the bottom of the Red Sea (Bischoff, 1969). Through time a 20 m thick succession of bedded mineral facies has been deposited. The most recent facies, a 5 m bed, apparently forming at present, is composed dominantly of an iron smectite with composition and structure intermediate between nontronite and the as yet undescribed trioctahedral ferrous iron smectite.

PHYSICAL PROPERTIES

The smectite bearing facies is characterized as a dark brown "soupy" mud of approximately 5 m thickness distributed over an area of 56 km^2. Interstitial brine contents are very high ranging from 85 to 96% on wet weight basis. The smectite accounts for approximately 75% of the solids with the rest being amorphous iron hydroxide with minor amounts of detrital pelagic carbonate.

The mineral occurs in birefringent colloidal particles displaying apple green color, and refractive indices of $1{\cdot}60 \pm 0{\cdot}005$.

SAMPLE PREPARATION

Bulk samples were collected from the four following cores taken from the geothermal area: 120K, 126P, 127P, and 128P (see Bischoff, 1969 for locations).

Due to significant impurities of amorphous iron hydroxide and detrital carbonates, leaching of the samples was necessary. The possibility that such a leaching treatment may attack and modify the mineral itself is recognized; analyses were, therefore, performed on the untreated bulk samples, and on the leached residues, to allow a monitor of the components lost during leaching.

The samples were first suspended in distilled water and placed in an ultrasound bath to remove interstitial brine, followed by drying at room temperature. One split was taken as representative of the original bulk material. The remaining sample was then treated with EDTA for carbonate dissolution followed by buffered dithionite solution described by Mehra and Jackson (1958) to remove iron hydroxide. This latter step probably attacked some of the smectite itself, but it is believed judging from the X-ray and chemical data (Figs. 1, 2 and Tables 1, 2, 5), that no significant restructuring took place. Microscopic examination indicated that all carbonate and ferric hydroxide had been removed during leaching, and that only the clay phase remained.

X-RAY DIFFRACTION

Following the methods outlined by Hathaway (1956), oriented mounts of both treated and untreated sodium saturated samples were scanned, and re-scanned subsequent, respectively, to glycolation, and heating to 400° and 550°C (Fig. 1). In addition powder camera photographs were taken (Table 5). Since all samples gave essentially identical patterns only 128P is presented.

Both sets of patterns are characteristic of smectite (MacEwan, 1961) with basal spacings of approximately 13·5 Å expanded by glycolation to about 15·5 Å, and collapsing to approximately 9·5 Å after heating. Moreover, peak positions for the leached and unleached samples are the same, the only difference being that in the former, intensity is greater.

In order to determine the (060) spacing, samples were subjected to low compressional stress in a hydraulic press, and diffractometer scans in the region of 60°2θ were performed on sections cut

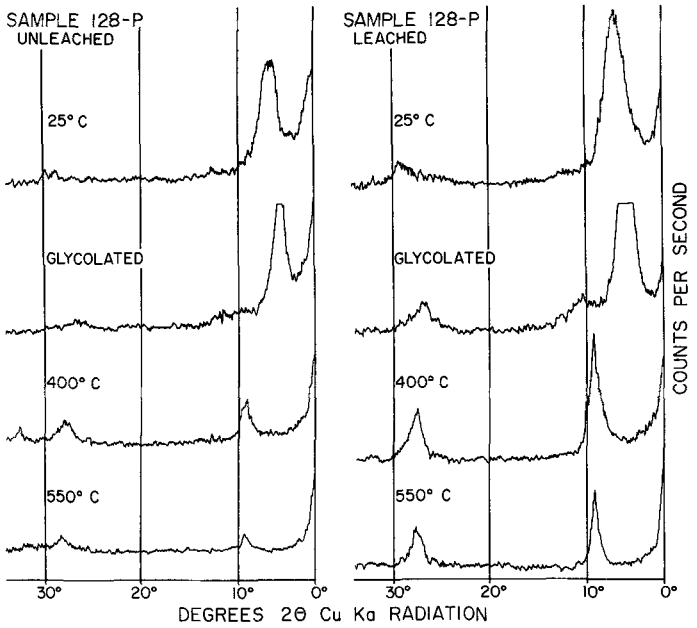

Fig. 1. X-ray diffractometer traces of Red Sea montmorillonite. Instrument settings as follows: Cu$K\alpha$ radiation, 2°/min scanning rate, 1000 counts/sec, full vertical scale between traces. Samples were oriented mounts on microporous silver filters. A graphite curved crystal monochrometer was used to discriminate against secondary Fe fluorescence from the sample.

perpendicular to the stress axis. (060) spacings of all samples are close to 1·53 Å, reflecting the partial trioctahedral character of the mineral, and high ferric in tetrahedral positions. (060) spacing for typical trioctahedral smectites are from 1·52 to 1·55 Å and for pure nontronites 1·522 Å (MacEwan, 1961).

CHEMICAL COMPOSITION

Chemical analyses were performed on both sets of samples by several methods. SiO_2 was determined colorimetrically by the acid molybdate technique (Bennett and Hawley, 1962), and FeO by titration with dichromate (Kolthoff and Sandell, 1952). The remaining metals (total Fe, Mn, Mg, Ca, Na, K, Cu and Zn) were determined by both atomic absorption spectroscopy and emission spectroscopy (pellet spark technique using borate fusion and internal standards (see Landergren, *et al.*, 1964). Ignition loss at 1000°C includes structural water, carbonate (as CO_2), reduced sulfur species (as SO_2), and gain by oxidation of ferrous iron.

A comparison of analytical results between leached and unleached samples (Tables 1 and 2) indicates an increase in SiO_2 and a decrease in Fe_2O_3, and CaO, as would be expected by removal of amorphous iron hydroxide and calcium carbonate. The increase in Na_2O after leaching indicates Na to be the major interlayer ion as might be expected of a clay formed in a saturated NaCl brine. Some Na, however, may have been added from the EDTA and dithionite during leaching. Later analysis of FeO yielded somewhat lower values indicating slow oxidation of the mineral while in contact with air.

Table 1. Chemical composition of Red Sea montmorillonite untreated samples

	120K	126P	127P	128P
SiO_2	27·3	29·3	30·9	28·9
Al_2O_3	2·1	1·9	1·8	1·9
Fe_2O_3	28·43	32·88	32·18	32·42
FeO	4·74	6·96	4·10	3·93
Mn_3O_4	0·80	0·35	1·70	0·80
MgO	1·21	0·81	1·40	1·28
CaO	4·50	1·8	7·0	6·7
Na_2O	0·55	0·65	0·83	0·97
K_2O	1·3	0·5	0·3	0·8
CuO	0·82	1·01	0·80	0·50
ZnO	1·7	5·5	2·7	2·2
Ignition loss	24·9	19·7	18·1	20·9
Total	98·35%	101·36%	101·81%	101·30%

https://doi.org/10.1346/CCMN.1972.0200406 Published online by Cambridge University Press

Table 2. Chemical composition of Red Sea montmorillonite samples treated with EDTA and dithionate

	120K	126P	127P	128P
SiO_2	36·4	38·1	39·0	32·9
Al_2O_3	2·1	2·8	2·6	2·3
Fe_2O_3	26·16	22·92	23·05	30·51
FeO	4·75	7·67	5·9	3·14
Mn_3O_4	1·2	0·04	0·36	0·32
MgO	1·5	0·97	1·28	1·30
CaO	0·5	0·2	0·5	0·5
Na_2O	2·8	2·3	2·7	3·03
K_2O	0·3	0·6	1·4	0·8
CuO	0·8	1·3	1·0	0·53
ZnO	1·9	4·8	2·6	2·1
Ignition loss	20·3	17·9	17·5	21·5
Total	98·71%	99·6%	97·89%	98·93%

Atomic proportions were calculated for the leached samples (Table 3) by taking the general smectite formula as $Y_{4-6}Z_8O_{20}(OH)_4 . nH_2O$ (MacEwan, 1961), where Y and Z refer to octahedrally and tetrahedrally coordinated cations respectively. As the amount of interlayer water is variable, atomic proportions were assigned on the basis that combined metal equals forty-four equivalents per formula unit.

After assigning all Si and Al from Table 2 to tetrahedral sites, the deficiency (Table 3) was assigned to ferric iron for a sum of 8 tetrahedral ions. Remaining ferric iron was assigned to octahedral sites, along with ferrous iron and Mn, Zn, Cu and Mg, all which have ionic radii suitable for octahedral coordination. The sum of these octahedral ions falls within the theoretical 4–6. Ferrous and ferric iron dominate the octahedral sites. The remaining ions, Ca, Na, and K, were then assigned to the interlayer exchangeable positions, for which Na is by far the most important.

The number of exchangeable ion equivalents (1·00 to 1·61, Table 3) indicates a cation exchange capacity in the range of 95–133 meq per 100 g. Significant amounts of occluded salts can be discounted as a source of the Na since leaching resulted in an increase in concentration.

The measured exchange capacities appear somewhat lower than those calculated from the structural formulae using K, Na and Ca (Table 4), by approximately 25%. Now, if potassium were fixed, it would not contribute to the measured capacity.

Table 4. Cation exchange capacities, calculated and experimental

meq/100g	120K	126P	127P	128P
Calculated from chemical analyses (including potassium)	113	93	134	131
Calculated, subtracting potassium	107	81	104	114
*Experimental	95	76	75	96

*Analyst: H. C. Starkey, U.S.G.S., Denver, using NH_4Cl to displace exchangeable ions.

Table 3. Atomic proportions calculated for treated samples

No. of ions		120K	126P	127P	128P
Tetrahedral sheets	Si	6·74	6·86	7·01	6·29
	Al	0·46	0·59	0·54	0·52
	Fe^{3+}	0·80	0·55	0·45	1·19
	Total	8·00	8·00	8·00	8·00
Octahedral sheets	Fe^{3+}	2·84	2·55	2·66	3·19
	Fe^{2+}	0·73	1·15	0·88	0·49
	Mn	0·18	—	0·05	0·05
	Zn	0·41	0·63	0·35	0·30
	Cu	0·11	0·17	0·14	0·08
	Mg	0·41	0·26	0·35	0·37
	Total	4·68	4·76	4·43	4·48
Interlayer	1/2 Ca	0·18	0·06	0·19	0·20
	Na	1·00	0·80	0·94	1·10
	K	0·07	0·14	0·32	0·18
Total interlayer charge		+1·25	+1·00	+1·45	+1·48
Octahedral and tetrahedral excess charge		−1·06	−1·07	−1·47	−1·56

https://doi.org/10.1346/CCMN.1972.0200406 Published online by Cambridge University Press

When potassium is subtracted from the calculated capacities (Table 4), agreement with experimental values becomes acceptable.

The excess tetrahedral and octahedral charge which gives rise to the cation exchange capacity is somewhat large, but is in the range for smectites. However, the tendency to fix potassium and form the mineral glauconite must be rather strong, and will probably take place with time.

The amount of tetrahedrally coordinated ferric iron (0·45–1·19 atoms, Table 3) is not unreasonable, and compares with 0·77 atoms of tetrahedral ferric iron found by Osthaus (1953) for the Garfield, Washington nontronite.

The number of octahedrally coordinated ferrous iron atoms (0·49–1·15 atoms, Table 3) should be taken as a minimum, since slow oxidation is probably taking place during sample storage. However, octahedral cations total between 4·43 and 4·76 (Table 3), so the mineral is nearer to being dioctahedral than trioctahedral.

Table 5. Powder camera data for sample 128P. Conditions: FeK_α radiation, 40 kv, 9 ma, 16 hr exposure, Mn filter.

Untreated sample			Treated sample		
d (Å)	I/I_1	hkl	d (Å)	I/I_1	hkl
13·77	100	001	13·89	100	001
7·63	5	—			
6·10	5	—			
4·59	25	003	4·63	25	003
4·28	10	—			
3·66	5	—			
3·36	30	004?	3·37	25	004?
3·04	30	—	3·03	5	—
2·83	25	—	2·86	5	—
1·531	5	060	1·538	5	060

In summary, the structure is characterized dominantly by Fe^{2+} and Fe^{3+} iron in the octahedral sites, and Si and Fe^{3+} in the tetrahedral sites. This structural composition is, therefore, intermediate between true dioctahedral nontronite and a trioctahedral hypothetical end member in which ferrous iron occupies all octahedral sites. Of the smectites reported in the literature, the mineral is similar in Fe^{2+} content to griffithite ($Fe^{2+}_{1.04}$, MacEwan, 1961), but which is dominated by Mg in the octahedral sites ($Mg_{3.76}$) and lacks tetrahedral Fe^{3+}.

MÖSSBAUER DATA

Mössbauer spectroscopy has become increasingly useful in the study of coordination and valence of iron in crystals (see Weaver *et al.*, 1967; Taylor *et al.*, 1968).

Mössbauer spectra on both sets of samples were kindly determined by Dr. Carol Herzenberg of the IIT Research Institute (Fig. 2). Both unleached and leached samples displayed similar patterns, the only difference being enhanced peak intensity (but unimproved resolution) in the latter. The patterns are characterized by a series of imperfectly resolved peaks in the region of approximately −0·5 mm/sec to +1·0 mm/sec, and a resolved peak in the region of +2·0 to 2·5 mm/sec, measured with respect to the center of metallic iron spectrum.

Mössbauer spectra presented by Weaver *et al.* (1967) with values adjusted to the convention used

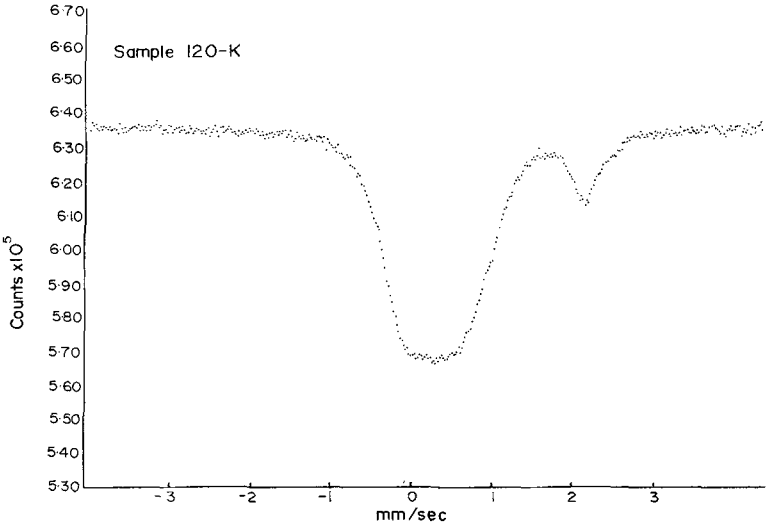

Fig. 2a.

https://doi.org/10.1346/CCMN.1972.0200406 Published online by Cambridge University Press

in this work, indicate that geothite (probably closely analogous to the amorphous $Fe(OH)_3$ in this work) displays a Fe^{3+} quadruple doublet at $+0{\cdot}1$ and $+0{\cdot}65$ mm/sec, while nontronite displays a single peak with an apex at $+0{\cdot}35$ mm/sec. Thus, a combination of these two minerals would yield unresolved broad peaks in the region near $+0{\cdot}2$ mm/sec. Spectra on biotite containing only ferrous iron in the octahedral sites indicate peaks at $-0{\cdot}5$ and 2·35 mm/sec. Octahedral Fe^{3+} in griffithite displays a doublet at $-0{\cdot}2$ mm/sec and $+1{\cdot}0$ mm/sec.

A spectrum of a biotite containing both octahedral and tetrahedral Fe^{3+} displays an additional peak at $+0{\cdot}45$ mm/sec which is attributed to tetrahedral iron.

Therefore, if the crystal chemistry deduced from the chemical data for the smectite is correct, and assuming iron in biotite is structurally analogous to that for the smectite, the Mössbauer spectrum would be expected to display peaks at $-0{\cdot}2$ and $+1{\cdot}0$ mm/sec for the octahedral Fe^{3+}, and $-0{\cdot}35$ and $+0{\cdot}45$ mm/sec for tetrahedral Fe^{3+}, plus peaks in the vicinity of $-0{\cdot}05$ and $+2{\cdot}35$ mm/sec for

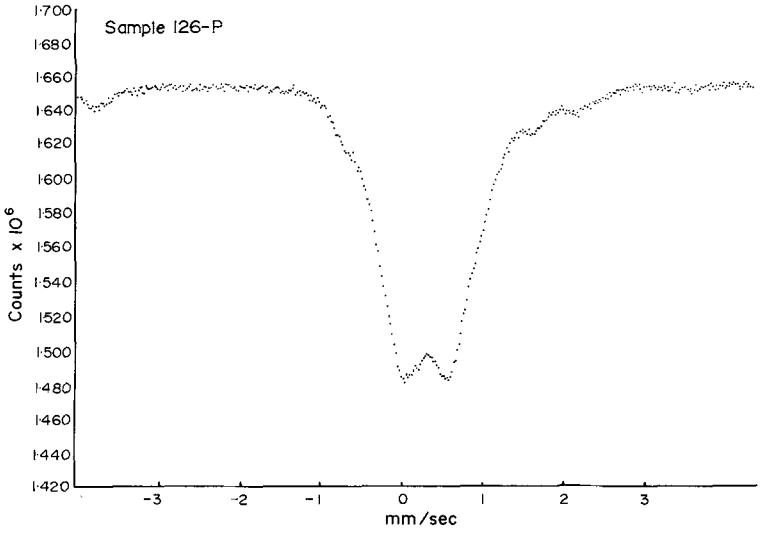

Fig. 2b.

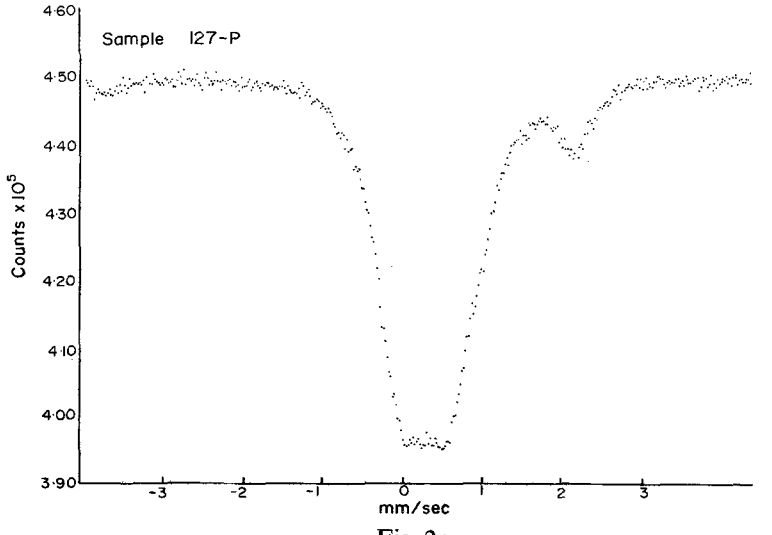

Fig. 2c.

https://doi.org/10.1346/CCMN.1972.0200406 Published online by Cambridge University Press

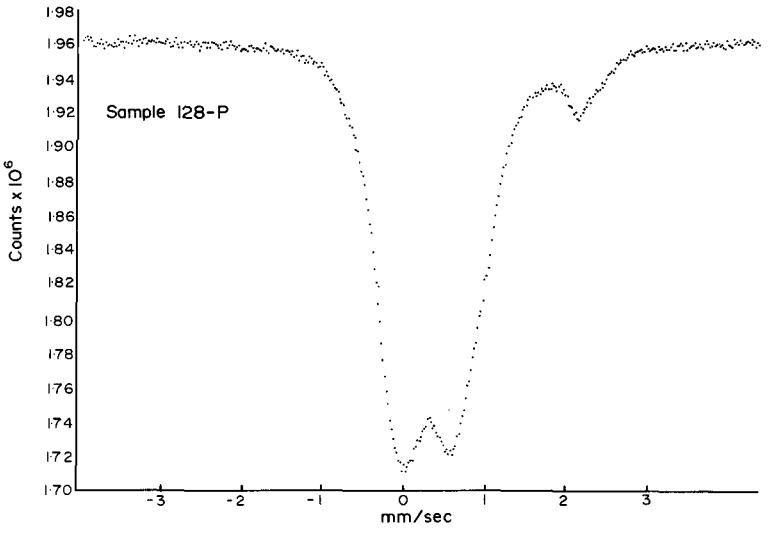

Fig. 2d.

Fig. 2. Mössbauer spectra of untreated Red Sea montmorillonite. Intensity is in units of total counts for the given scan period; abscissa in velocity units measured from center of metallic iron spectrum. Analyst: Caroline L. Herzenberg, IIT Research Institute. (a) Sample 120K, 5 hr scan; (b) Sample 126P, 16 hr scan; (c) Sample 127P, 4 hr scan; (d) Sample 128P, 16 hr scan.

octahedral Fe^{2+}. The peaks between $-0{\cdot}35$ and $+1{\cdot}0$ would be unresolved, resulting in a somewhat broad peak with perhaps some apices displayed. The peak in the vicinity of $+2{\cdot}3$ mm/sec due specifically to octahedral Fe^{2+} would be resolved. The peaks for the $Fe(OH)_3$ impurity would fall unresolved in the region of $-0{\cdot}35$ and $+1{\cdot}0$ mm/sec. The patterns in Figs. 2a–d are seen to be consistent with this model, and serve to establish that ferrous iron is indeed in the octahedral sites of the clay.

GENESIS

The precipitation mechanism for the mineral apparently requires a combination of cooling of the brine, and subsequent mixing with the Red Sea bottom waters. All components appear to come from the brine, which contains approximately 60 ppm dissolved SiO_2 and 80 ppm Fe^{2+}, as well as the other heavy metal components (Brewer and Spencer, 1969). As the brine discharges on the sea floor, it cools thereby making dissolved silica supersaturated. During mixing with seawater, a portion of Fe^{2+} is oxidized, and the smectite precipitates as a mixture dominantly of Fe^{2+}, Fe^{3+} and SiO_2. After precipitation in the water column, the material settles to the sea floor. The mineral is most likely unstable in the presence of sea water, and a trend toward equilibrium would probably involve K fixation and formation of glauconite.

Acknowledgments—I wish to express my thanks to Dr. Caroline L. Herzenberg of IIT Research Institute who generously performed the Mössbauer analyses, assisted in their interpretation, and provided helpful discussion and suggestions. Powder camera photographs and exchange capacity determinations were performed by Harry C. Starkey of the U.S. Geological Survey for which I am most grateful. The manuscript was critically read and improved by John C. Hathaway, who also provided the initial encouragement to carry out the study. Financial support was from the American Chemical Society, Petroleum Research Fund, Grant No. 5107-AC2.

REFERENCES

Bennet, H. and Hawley, W. G. (1965) *Methods of Silicate Analysis*, 2nd Edn, 334 pp., Academic Press, New York.

Bischoff, J. L. (1969) The Red Sea Geothermal deposits: Their mineralogy, chemistry, and genesis: In *Hot Brines and Recent Heavy Metal Deposits in the Red Sea* (Edited by Degens, E. T., and Ross, D.), pp. 368–401, Springer, New York.

Brewer, P. G. and Spencer, D. W. (1969) A note on the Chemical Composition of the Red Sea Brines: In *Hot Brines and Recent Heavy Metal Deposits in the Red Sea* (Edited by Degens, E . T ., and Ross, D .), Springer, New York.

Grim, R. E. (1968) *Clay Mineralogy*, 2nd Edn, 596 pp., McGraw-Hill, New York.

Hathaway, J. C. (1956) Procedures for clay mineral analyses used in the sedimentary petrology laboratory

of the U.S. Geological Survey: *Clay Minerals Bull.*, **3**, 8–13.

Kolthoff, I. M. and Sandell, E. B. (1952) *Textbook of Quantitative Inorganic Analysis*, 3rd Edn, 859 pp., Macmillan, New York.

MacEwan, D. M. C. (1961) Montmorillonite minerals: In *The Identification and Crystal Structure of Clay Minerals* (Edited by Brown, G.), pp. 132–142, Mineralogical Soc., London.

Mehra, O. P., and Jackson, M. L. (1958) Iron oxide removal from soil and clays by a dithionite–citrate system buffered with sodium bicarbonate: *Clays and Clay Minerals* **5**, 317–327.

Osthaus, B. B. (1953) Chemical determination of tetrahedral ions in nontronite and montmorillonite: *Clays and Clay Minerals* **2**, 404–417.

Taylor, G. L., Ruotsals, A. E. and Keeling, Jr., R. O. (1968) Analysis of iron in layer silicates by Mössbauer spectroscopy: *Clay and Clay Minerals* **16**, 381–391.

Weaver, C. E., Wampler, J. M. and Pecuil, T. E. (1967) Mössbauer analysis of iron in clay minerals: *Science* **156**, 504–508.

Résumé—Une smectite riche en fer ferreux et pauvre en aluminium est abondamment rencontrée dans les dépôts géothermaux de la Mer Rouge, et il apparaît qu'elle se forme actuellement.

Les analyses chimiques et les spectres Mössbauer indiquent que ce minéral a une composition intermédiaire entre celle de la nontronite et celle du terme ultime de la série trioctaédrique à fer ferreux non encore décrit.

Kurzreferat—Ein Smectit (Seifenstein) reich an Ferro-Eisen und mit niedrigen Aluminiumgehalt kommt reichlich vor in den geothermischen Ablagerungen des Roten Meeres.

Chemische Analyse und Mössbauer Spektren zeigen an, dass das Mineral in seiner Zusammensetzung eine Mittelstellung zwischen Nontronit und dem bisher nicht beschriebenen trioktaedrischen Ferro-Eisen-Endglied einnimmt.

Резюме — Смектит, богатый примесью двухвалентного железа и с низким содержанием алюминия, находится в изобилии в геотермических отложениях Красного моря и, кажется, образовывается даже в настоящее время.

Химические анализы и спектры Моссбауера указывают, что этот минерал является промежуточным продуктом между нонтронитом и еще неописанным конечным элементом решетки трехоктаэдральным двухвалентным железом.